REAL-TIME GUITAR TUBE AMPLIFIER SIMULATION USING AN APPROXIMATION OF DIFFERENTIAL EQUATIONS

Jaromir Macak

Dept. of Telecommunications,
FEEC, Brno University of Technology
Brno, Czech Republic
`jaromir.macak@phd.feec.vutbr.cz`

Jiri Schimmel

Dept. of Telecommunications,
FEEC, Brno University of Technology
Brno, Czech Republic
`schimmel@feec.vutbr.cz`

ABSTRACT

Digital simulation of guitar tube amplifiers is still an opened topic. The efficient implementation of several parts of the guitar amplifier is presented in this paper. This implementation is based on the pre-computation of the solution of the nonlinear differential system and further approximation of the solution. It reduces the computational complexity while the accuracy is comparable with the numerical solution. The method is used for simulation of different parts of the guitar amplifier, namely a triode preamp stage, a phase splitter and a push-pull amplifier. Finally, the results and comparison with other methods are discussed.

1. INTRODUCTION

Recently, there has been extensive research in the field of digital simulation of analog guitar effects and amplifiers and several algorithms for real-time simulation has been proposed [1]. Fundamentally, all circuit simulation-based algorithms use a block decomposition, which allows description of each block more precisely. The static waveshaping and linear filtration algorithm presented in [2] provides good results for stationary signals but fails on transients because of the dynamic bias changes that appear in analog circuits. The major advantage of this algorithm is its speed if a nonlinearity is implemented as the look-up table or approximated via linear or spline interpolation.

Nonlinear wave digital filters (WDF) offer efficient and dynamic simulation of circuits with one nonlinear function (more nonlinearities typically decrements efficiency). The diode limiter unit is simulated in [3] and the simulation of common-cathode triode amplifier with no grid current is presented in [4]. The WDF are very efficient if the circuit is linear or if there are one [4] or two [5] nonlinear functions. However, the guitar amplifier circuits can contain more nonlinear functions.

Numerical methods for simulation of the nonlinear diode limiter unit are described in [6]. They are based on a numerical solution of the nonlinear differential equations (ODE) and it is possible to use this method for simulation of more complicated circuits with more nonlinear functions. A similar approach is used in professional circuit schematic simulators (e.g., SPICE) where the nonlinear circuit equations are in matrix form and LU decomposition is used for solving the system. The major disadvantage is its computational complexity.

A common-cathode triode amplifier with a nonlinear grid and plate currents, a triode phase splitter and a pentode push-pull amplifier are described using nonlinear ODEs in this paper. Subsequently, the Euler method is applied for the ODEs. The solution of

the ODEs depends on an input signal voltage and on a circuit state (capacitor voltages). Therefore, the described system is considered to have more inputs. To reduce the computational complexity, the solution of the ODEs is pre-computed and approximated for the combination of different inputs (the input signal and the capacitor voltages). The approximated values can be used for one iteration of the Newton-Rapson method as an estimation or directly as output signal values if the step of input voltages is small enough. Furthermore, the stability of the solution is guaranteed if the input voltages are within the approximated range.

2. BLOCK DIAGRAM OF THE GUITAR TUBE AMPLIFIER

A typical guitar tube amplifier is shown in Figure 1. The preamp consists of several common-cathode triode amplifiers with different values of circuit elements, a cathode follower and a tone stack circuit. The power amplifier contains a phase splitter, a push-pull amplifier, an output transformer and a global negative feedback.
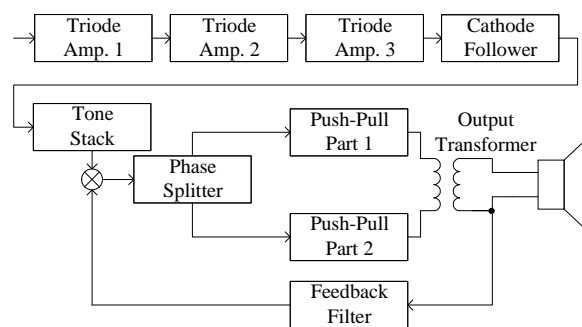

Figure 1: Block diagram of a typical guitar tube amplifier.

Several simplifications will be introduced in this simulation:

- the simulation is divided into blocks,
- the preamp power supply is constant,
- the cathode follower is ideal impedance divider,
- the tone stack is the digital filter designed according to [7],
- the output transformer is ideal,
- the power amplifier load is constant,
- an extra delay block in the feedback to avoid the delay free loop.

3. NONLINEAR TUBE MODELS

The accuracy of the simulation is related to the chosen simulation algorithm as well as with the nonlinear device models. Koren's model is used in this paper [8].

The triode plate current is given by

$$I_a = \frac{E_1^{E_x}}{K_{g1}}(1 + \text{sgn}(E_1)) \tag{1}$$

where

$$E_1 = \frac{U_{ak}}{K_p} \log(1 + \exp(K_p(\frac{1}{\mu} + \frac{U_{gk}}{\sqrt{K_{vb} + U_{ak}^2}}))). \tag{2}$$

Parameters μ, E_x, K_{g1}, K_{g2}, K_p and K_{vb} are listed in table 1, U_{gk} is the grid-to-cathode voltage and U_{ak} is the plate-to-cathode voltage. The pentode plate current is given by

$$I_a = \frac{E_1^{E_x}}{K_{g1k}}(1 + \text{sgn}(E_1)) \arctan(\frac{U_{ak}}{K_{vb}}), \tag{3}$$

where

$$E_1 = \frac{U_{g2k}}{K_p} \log(1 + \exp(K_p(\frac{1}{\mu} + \frac{U_{g1k}}{U_{g2k}}))) \tag{4}$$

and the pentode screen current is given by

$$I_s = \frac{\exp(E_x \log(\frac{U_{g2k}}{\mu} + U_{g1k}))}{K_{g2}}. \tag{5}$$

Voltage U_{g1k} is the pentode grid-to-cathode voltage and U_{g2k} is the screen-to-cathode voltage. The grid current is not specified in [8], therefore the grid model was adopted from SPICE simulator. The grid current is

$$I_g = \begin{cases} g_{cf}(u_{gk} - g_{co})^{3/2} & u_{gk} \geq g_{co} \\ 0 & u_{gk} < g_{co} \end{cases} \tag{6}$$

where $g_{cf} = 1 \cdot 10^{-5}$ and $g_{co} = -0,2$.

Tube	μ	E_x	K_{g1}	K_{g2}	K_p	K_{vb}
12AX7	100	1.4	1060	-	600	300
6L6GC	8.7	1.35	1460	4500	48	12
EL34	11.0	1.35	650	4200	60	24

Table 1: Model parameters for different tubes.

4. TRIODE AMPLIFIER SIMULATION

A triode amplifier circuit can be found in each guitar preamplifier. An example of the common-cathode triode amplifier circuit is shown in Figure 2. This circuit is described using the nonlinear differential system

$$0 = G_2 \frac{U_{in}G_1 + U_g G_2}{G_1 + G_g + G_2} - U_g G_2 - i_g$$
$$0 = U_k G_k - i_a - i_g + C_k \frac{dU_k}{dt} \tag{7}$$
$$0 = U_N G_a - U_a G_a - U_a G_L - i_a$$

where ig is grid current $i_g(U_g - U_k)$ and i_a is plate current $ia(U_g - U_k, U_a - U_k)$. The symbol G represents the conductance of the resistors from the circuit schematic in Figure 2. The differential system consists of the three unknown variables U_g, U_k, U_a and the output signal value can be derived directly from the voltage U_a.
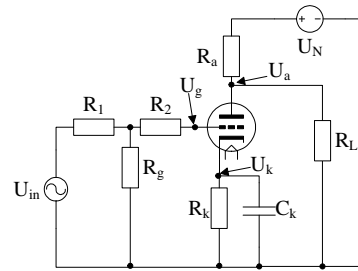

Figure 2: *Triode amplifier circuit schematic ($R_1 = 68\,\text{k}\Omega$, $R_2 = 1\,\Omega$, $R_g = 1\,\text{M}\Omega$, $R_k = 2.7\,\text{k}\Omega$, $R_a = 100\,\text{k}\Omega$, $R_L = 4\,\text{M}\Omega$, $C_k = 680\,\text{nF}$ and $U_N = 350\,\text{V}$).*

4.1. Approximation of Differential equations

Using the Euler method

$$y_{n+1} = y_n + T_s f(y_{n+1}) \tag{8}$$

with the sampling period T_s for the system (7) leads to a system

$$0 = G_2 \frac{U_{in}G_1 + U_g G_2}{G_1 + G_g + G_2} - U_g G_2 - i_g$$
$$0 = U_{c1m} - U_c - \frac{U_k G_k - i_a - i_g}{C_k f_s} \tag{9}$$
$$0 = U_N G_a - U_a G_a - U_a G_L - i_a$$

that consists of unknown variables U_g, U_k, U_a, the capacitor voltage U_{c1m} from the last sample period and the input signal voltage U_{in}. This means that the system contains two inputs U_{km} and U_{in}. The unknown variables U_g, U_k, U_a can be numerically computed for the different combinations of the inputs and then can be approximated as the functions of two input variables

$$U_g = U_{Gapprox}(U_{in}, U_{c1m})$$
$$U_k = U_{Kapprox}(U_{in}, U_{c1m}) \tag{10}$$
$$U_a = U_{Aapprox}(U_{in}, U_{c1m}).$$

The approximated functions of plate and grid voltages are depicted in Figures 3 and 4.
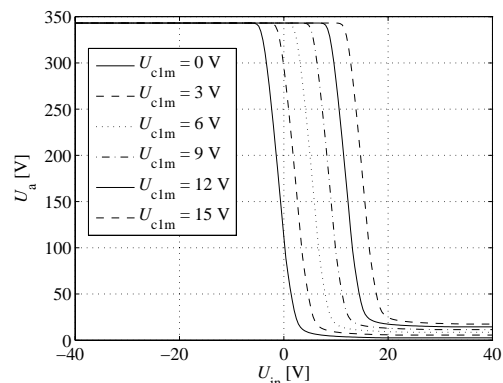

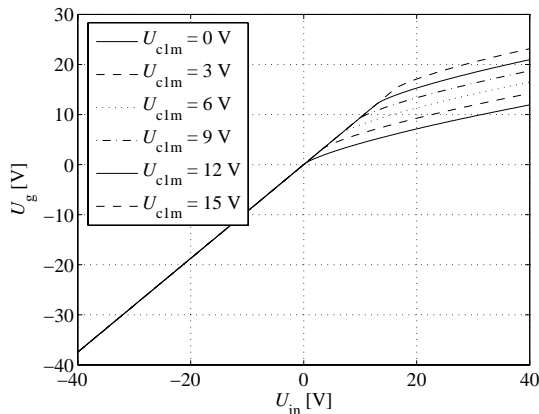Figure 3: *Plate voltage functions on different capacitor voltage.*

Figure 4: *Grid voltage functions on different capacitor voltage.*

Once the functions are approximated, the simulation process starts. Firstly, the DC voltages are computed, then the voltages U_g, U_k, U_a are computed from (10). The last step is computation of the new capacitor voltage used in next sample period. The capacitor voltage can be obtained from

$$U_{c1m}[n+1] = U_{c1m}[n] - \frac{U_k G_k - i_a - i_g}{C_k f_s} \qquad (11)$$

where the currents i_g and i_a are computed from the approximated voltages U_g, U_k, U_a.

4.2. Simulation Results

The output voltage for the 1kHz sinewave input with an amplitude of 5 V at a sampling frequency of 96 kHz is displayed in figure 5 and compared to the solution without the approximation. The
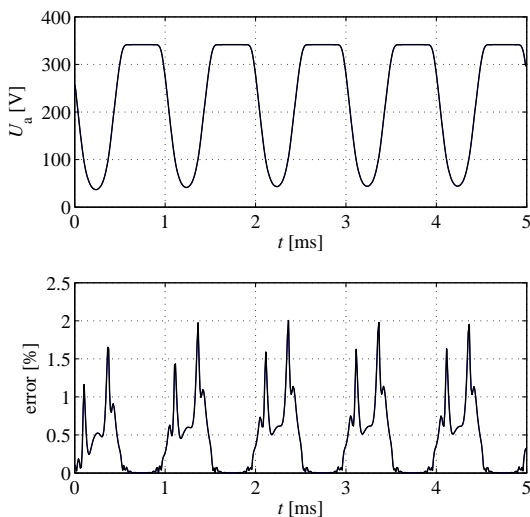

Figure 5: *The output (top) and error (bottom) signal of the simulated triode amplifier.*

smaller the step is, the better-obtained accuracy. The step of 2 V for the input voltages and the cubic spline interpolation were used. Figure 6 shows the sine sweep log spectogram and frequency response of the triode amplifier. The gain is reduced at low frequencies due to the negative cathode feedback. The frequency response is distorted at the frequencies close to the Nyquist frequency due to bilinear transform warping.
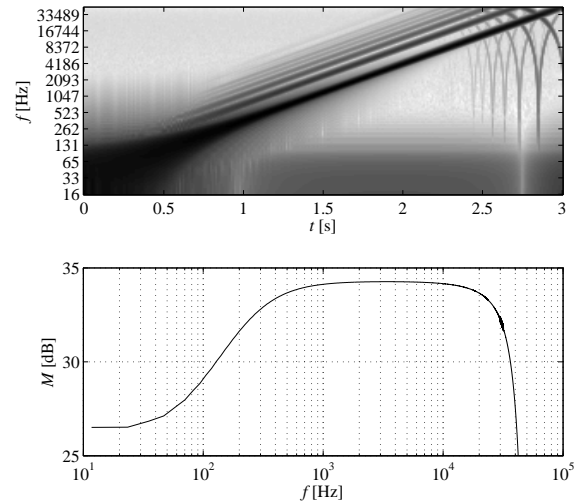

Figure 6: *Sine sweep log spectogram (top) and frequency response (bottom) of the simulated triode amplifier.*

5. SIMULATION OF TRIODE AMPLIFIER CONNECTED IN SERIES

The simulation of the single triode amplifier does not count on the influence of adjacent blocks, therefore it can be used only as the input triode stage, where the signal is small enough and there is no grid current flowing to the next triode. For larger input signals, the grid current of adjacent blocks has to be taken into account. This nonlinear current shifts the bias of the next triode amplifier by discharging of the decoupling capacitor and also compresses the output signal due to increasing R_a voltage. The influence of the grid current of an adjacent triode amplifier to the transfer function is shown in Figure 7 where the second triode grid current is related to the different load of the first triode amplifier.
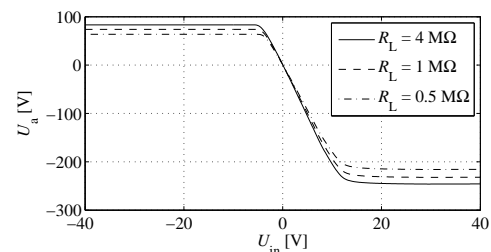

Figure 7: *The influence of the grid current of an adjacent triode amplifier to the transfer function of triode amplifier.*

In order to simulate the bias shift and the compression, the coupling of triode amplifiers has to be simulated together. The output voltage is obtained from the output of the first triode in the first couple and then is used as the input of next couple. It is supposed that the third triode connected to the output of the second triode in the couple has minimal influence on the first tube of the coupling. Thus, the second triode of the couple works into a constant load. The whole process of block decomposition is illustrated in Figure 8 where the preamplifier containing four triodes is replaced with three couples of triodes. This process of decomposition allows the simulation of the adjacent blocks interaction. However, it increases the computational complexity.
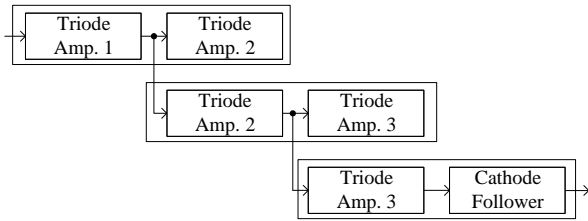

Figure 8: *Preamp block decomposition.*

Figure 9 shows the circuit schematic of the couple of triodes. The second triode amplifier builds the nonlinear load for the first one. The output signal is obtained from the output of the capacitor C_a. The ODEs of the couple of triodes are

$$0 = G_2 \frac{U_{\text{in}} G_1 + U_{\text{g}} G_2}{G_1 + G_{\text{g}} + G_2} - U_{\text{g}} G_2 - i_{\text{g}}$$

$$0 = U_{\text{k}} G_{\text{k}} - i_{\text{a}} - i_{\text{g}} + C_{\text{k}} \frac{dU_{\text{k}}}{dt}$$

$$0 = (U_{\text{N}} - U_{\text{a}}) G_{\text{a}} - i_{\text{a}} - (U_2 - U_{\text{g2}}) G_3$$

$$0 = C_{\text{a}} \frac{d(U_{\text{a}} - U_2)}{dt} - (U_2 - U_{\text{g2}}) G_3 \qquad (12)$$

$$0 = (U_2 - U_{\text{g2}}) G_3 - U_{\text{g2}} G_{\text{g2}} - i_{\text{g2}}$$

$$0 = U_{\text{k2}} G_{\text{k2}} - i_{\text{a2}} - i_{\text{g2}}$$

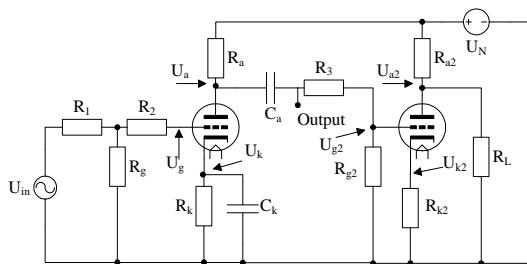$$0 = (U_{\text{N}} - U_{\text{a2}}) G_{\text{a2}} - U_{\text{a2}} G_{\text{L}} - i_{\text{a2}}.$$

Figure 9: *Circuit schematic of couple of triode amplifiers ($R_1 = 68\,\text{k}\Omega$, $R_2 = 1\,\Omega$, $R_{\text{g}} = 1\,\text{M}\Omega$, $R_{\text{k}} = 2.7\,\text{k}\Omega$, $R_{\text{a}} = 100\,\text{k}\Omega$, $R_3 = 470\,\text{k}\Omega$, $R_{\text{g2}} = 1\,\text{M}\Omega$, $R_{\text{k2}} = 10\,\text{k}\Omega$, $R_{\text{a2}} = 100\,\text{k}\Omega$, $R_{\text{L}} = 4\,\text{M}\Omega$, $C_{\text{k}} = 680\,\text{nF}$, $C_{\text{a}} = 22\,\text{nF}$ and $U_{\text{N}} = 350\,\text{V}$).*

5.1. Approximation of Differential Equations

The equations to be approximated are

$$0 = G_2 \frac{U_{\text{in}} G_1 + U_{\text{g}} G_2}{G_1 + G_{\text{g}} + G_2} - U_{\text{g}} G_2 - i_{\text{g}}$$

$$0 = U_{\text{c1m}} - U_{\text{c1}} - \frac{U_{\text{k}} G_{\text{k}} - i_{\text{a}} - i_{\text{g}}}{C_{\text{k}} f_{\text{s}}}$$

$$0 = (U_{\text{N}} - U_{\text{a}}) G_{\text{a}} - i_{\text{a}} - (U_2 - U_{\text{g2}}) G_3$$

$$0 = U_{\text{c2m}} - U_{\text{c2}} + \frac{(U_2 - U_{\text{g2}}) G_3}{C_{\text{a}} f_{\text{s}}} \qquad (13)$$

$$0 = (U_2 - U_{\text{g2}}) G_3 - U_{\text{g2}} G_{\text{g2}} - i_{\text{g2}}$$

$$0 = U_{\text{k2}} G_{\text{k2}} - i_{\text{a2}} - i_{\text{g2}}$$

$$0 = (U_{\text{N}} - U_{\text{a2}}) G_{\text{a2}} - U_{\text{a2}} G_{\text{L}} - i_{\text{a2}}.$$

The system has three inputs U_{in}, U_{cm1}, U_{cm2} and approximated functions are

$$U_{\text{g}} = U_{\text{Gapprox}}(U_{\text{in}}, U_{\text{c1m}}, U_{\text{c2m}})$$

$$U_{\text{k}} = U_{\text{Kapprox}}(U_{\text{in}}, U_{\text{c1m}}, U_{\text{c2m}})$$

$$U_{\text{a}} = U_{\text{Aapprox}}(U_{\text{in}}, U_{\text{c1m}}, U_{\text{c2m}}) \qquad (14)$$

$$I_{\text{R3}} = I_{\text{R1approx}}(U_{\text{in}}, U_{\text{c1m}}, U_{\text{c2m}}).$$

The capacitor voltages are recomputed using

$$U_{\text{c1m}}[n+1] = U_{\text{c1m}}[n] - \frac{U_{\text{k}} G_{\text{k}} - i_{\text{a}} - i_{\text{g}}}{C_{\text{k}} f_{\text{s}}} \qquad (15)$$

and

$$U_{\text{c2m}}[n+1] = U_{\text{c2m}}[n] + \frac{I_{\text{R3}}}{C_{\text{a}} f_{\text{s}}}. \qquad (16)$$

5.2. Simulation Results

Figure 10 shows the output signal of the coupling of triode amplifiers. The output signal is compared to the output signal from the single triode amplifier with the same schematic values. The positive voltage compression of the output signal appears in the coupled triode amplifier and also the capacitor voltage U_{cm2} is discharging because of the grid current of the second triode. This causes the bias change in the next triode couple.
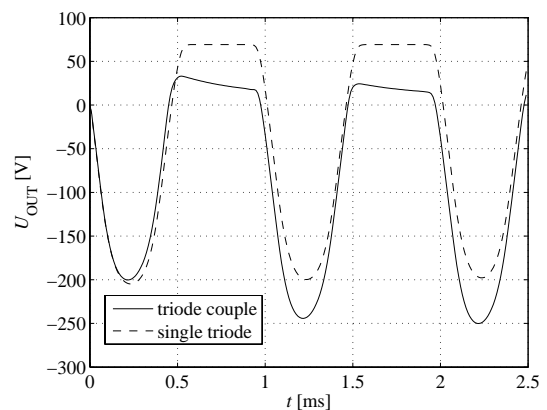

Figure 10: *Output signals comparison of single triode amplifier and couple of triodes.*

6. TRIODE PHASE SPLITTER SIMULATION

The triode phase splitter is used for amplification of the signal for the power amplifier tubes and for the inverted signal generation. The circuit schematic is displayed in Figure 11. The phase splitter is far from an ideal one, the inverted signal does not have the same amplitude as the direct signal and both the signals (direct and inverted) are nonlinearly distorted. The phase splitter block also has influence on the frequency response. The capacitors C_1 and C_2 build the high-pass filter and the combination of C_3 and R_4 emphasizes the middle frequencies by short-circuiting the negative global feedback on the resistor R_5. The negative feedback AC voltage is fed via capacitor C_2 to the grid of the second tube. To simplify the task, the negative feedback voltage can be fed to the grid of the fist tube with the opposite sign. This means that the direct and feedback signal can be summed in front of the phase splitter block. The feedback voltage in figure 11 is connected to the ground, which leads to ODEs

$$0 = (U_{\text{in}} - U_1)G_1 - (U_{\text{g1}} - U_2)G_{\text{g1}} - i_{\text{g1}}$$
$$0 = C_1\frac{d(U_1 - U_{\text{g1}})}{dt} - (U_{\text{in}} - U_1)G_1$$
$$0 = (U_{\text{k}} - U_2)G_{\text{k}} - i_{\text{a1}} - i_{\text{g1}} - i_{\text{a2}} - i_{\text{g2}}$$
$$0 = (U_{\text{N}} - U_{\text{a1}})G_{\text{a1}} - U_{\text{a1}}G_{\text{L1}} - i_{\text{a1}}$$
$$0 = (U_{\text{N}} - U_{\text{a2}})G_{\text{a2}} - U_{\text{a2}}G_{\text{L2}} - i_{\text{a2}}$$
$$0 = -i_{\text{g2}} + (U_2 - U_{\text{g2}})G_{\text{g2}} - C_2\frac{d(U_{\text{g2}} - U_3)}{dt} \quad (17)$$
$$0 = (U_{\text{g1}} - U_2)G_{\text{g1}} + (U_{\text{k}} - U_2)G_{\text{k}} -$$
$$\quad - (U_{\text{g}} - U_{\text{g2}})G_{\text{g2}} - (U_2 - U_3)G_2$$
$$0 = (U_2 - U_3)G_2 - U_3 G_3 - U_3 G_5 - U_4 G_4 +$$
$$\quad + C_2\frac{d(U_{\text{g2}} - U_3)}{dt}$$
$$0 = C_3\frac{d(U_3 - U_4)}{dt} - U_4 G_4.$$

The feedback signal goes through the feedback filter (see Figure 1) connected according to Figure 12 with the analog transfer function

$$H(s) = \frac{(R_4 R_5 C_3)s + R_5}{(C_3 R_4 R_5 + C_3 R_3 R_5 + C_3 R_3 R_4)s + R_3 + R_5}. \quad (18)$$

The resistor R_4 can often be found as the potentiometer "Presence". In this case, the intensity of the feedback can be changed with influence to the frequency response.

The transfer function (18) is discretized using bilinear transform resulting to discrete transfer function $H(z)$ and the feedback voltage U_{FDB} is obtained from the output of filter $H(z)$ with input signal U_{OUT}

$$U_{\text{FDB}}[n] = \mathcal{Z}^{-1}\left\{H(z)\mathcal{Z}\left\{U_{\text{OUT}}[n-1]\right\}\right\}. \quad (19)$$

The signal U_{OUT} is obtained at the output of the power amplifier (see equation (26)) and it is delayed one sample period due to elimination of the delay free loop. This simplification influences the frequency response of the power amplifier due to the different phase delay in the feedback. However, the input and output signals have to be oversampled to reduce aliasing distortion. Thus, the frequency distortion caused by the extra unit delay block manifests outside the audible region.
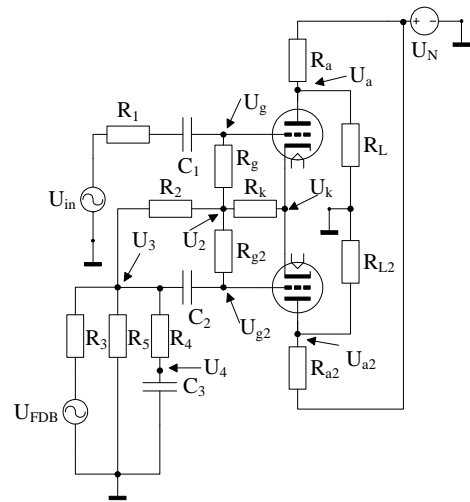

Figure 11: *Phase splitter circuit schematic ($R_1 = 1\,\Omega$, $R_{\text{g1,2}} = 1\,\text{M}\Omega$, $R_{\text{k}} = 470\,\Omega$, $R_2 = 10\,\text{k}\Omega$, $R_3 = 100\,\text{k}\Omega$, $R_4 = 22\,\text{k}\Omega$, $R_1 = 4.7\,\text{k}\Omega$, $R_{\text{a1}} = 82\,\text{k}\Omega$, $R_{\text{a2}} = 100\,\text{k}\Omega$, $R_{\text{L1,2}} = 4\,\text{M}\Omega$, $C_{1,2,3} = 100\,\mu\text{F}$ and $U_{\text{N}} = 400\,\text{V}$.)*
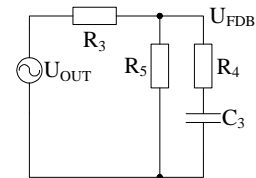

Figure 12: *Circuit schematic of the simplified feedback filter.*

6.1. Approximation of Differential Equations

The ODEs (17) are discretized using (8). The system has four inputs U_{in}, U_{cm1}, U_{cm2} and U_{cm3} and the approximated functions are

$$U_{\text{g1}} = U_{\text{G1approx}}(U_{\text{in}}, U_{\text{c1m}}, U_{\text{c2m}}, U_{\text{c3m}})$$
$$U_{\text{g2}} = U_{\text{G2approx}}(U_{\text{in}}, U_{\text{c1m}}, U_{\text{c2m}}, U_{\text{c3m}})$$
$$U_{\text{k}} = U_{\text{Kapprox}}(U_{\text{in}}, U_{\text{c1m}}, U_{\text{c2m}}, U_{\text{c3m}})$$
$$U_{\text{a1}} = U_{\text{A1approx}}(U_{\text{in}}, U_{\text{c1m}}, U_{\text{c2m}}, U_{\text{c3m}}) \quad (20)$$
$$U_{\text{a2}} = U_{\text{A2approx}}(U_{\text{in}}, U_{\text{c1m}}, U_{\text{c2m}}, U_{\text{c3m}})$$
$$U_2 = U_{\text{2approx}}(U_{\text{in}}, U_{\text{c1m}}, U_{\text{c2m}}, U_{\text{c3m}})$$
$$U_4 = U_{\text{4approx}}(U_{\text{in}}, U_{\text{c1m}}, U_{\text{c2m}}, U_{\text{c3m}}).$$

The capacitor voltages are recomputed using

$$U_{\text{c1m}}[n+1] = U_{\text{c1m}}[n] + \frac{(U_{\text{g1}} - U_2)G_{\text{g1}} + i_{\text{g1}}}{C_1 f_{\text{s}}} \quad (21)$$

and

$$U_{\text{c2m}}[n+1] = U_{\text{c2m}}[n] - \frac{(U_{\text{g2}} - U_2)G_{\text{g2}} + i_{\text{g2}}}{C_2 f_{\text{s}}} \quad (22)$$

and

$$U_{\text{c3m}}[n+1] = U_{\text{c3m}}[n] + \frac{U_4 G_4}{C_3 f_{\text{s}}}. \quad (23)$$

6.2. Simulation Results

The simulation of the triode phase splitter block was tested with 1 kHz sinewave input signal at a sampling frequency of 96 kHz and an amplitude of 8 V. The inverted signals U_{a1} and U_{a2} (see Figure 13) are nonlinearly distorted and have different amplitude as was expected. Figure 14 displays the frequency response of the tube power amplifier with different values of potentiometer R_4 (Presence). The maximal presence effect occurs (dash-dotted line) when the potentiometer R_4 has the lowest value and there is no negative feedback for higher frequencies. For the higher values of the potentiometer R_4, the negative feedback is constant for all frequencies. The high-pass filter effect is caused by C_1 and C_2 capacitors.
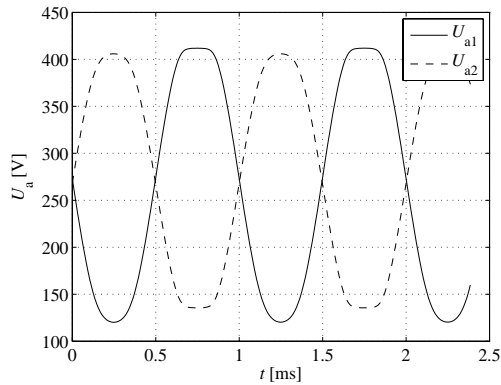

Figure 13: *Inverted and direct output signal of the phase splitter simulation for 1kHz sinewave input with an amplitude of 8 V at a sampling frequency of 96 kHz.*
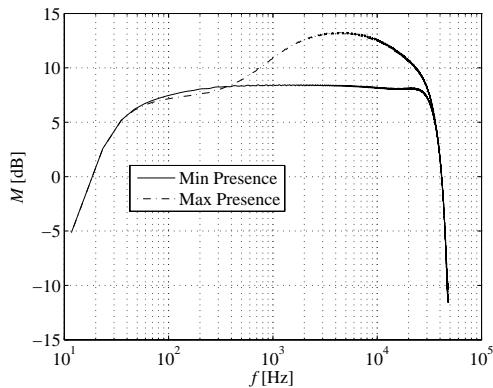

Figure 14: *Frequency response of the phase splitter for minimal value of R_4 (maximal presence effect) and maximal value of R_4 (minimal presence effect).*

7. OUTPUT POWERAMP SIMULATON

A typical guitar power amplifier consists of two or four pentodes connected in push-pull topology operating in class A or class AB. A simplified circuit schematic is displayed in Figure 15 and it can

be divided into two parts. The first one is the grid current circuit and the second one is the plate current circuit. The both parts are independent because there is no coupling via cathode resistor as with the triode amplifiers. The plate resistors R_a simulates the loudspeaker load transformed by the output transformer. It must be noted that a high level of simplification was used because the speaker load is frequency dependent and the output transformer is far from an ideal one. The resistor R_D simulates the rectifier resistance. It can be used for the simulation of a tube (higher values) or semiconductor rectifier (lower values). The combination of R_D and C_2 also simulates power amplifier compression (*sagging effect*).
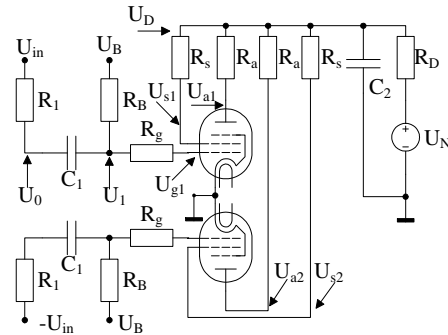

Figure 15: *Push-pull amplifier schematic ($R_1 = 30\,\mathrm{k\Omega}$, $R_B = 220\,\mathrm{k\Omega}$, $R_g = 5\,\mathrm{k\Omega}$, $R_a = 1.7\,\mathrm{k\Omega}$, $R_s = 1\,\mathrm{k\Omega}$, $R_D = 500\,\Omega$, $C_1 = 22\,\mathrm{nF}$, $C_2 = 100\,\mu\mathrm{F}$, $U_B = -50\,\mathrm{V}$ and $U_n = 450\,\mathrm{V}$).*

The grid voltages U_{g1} and U_{g2} are computed from

$$
\begin{aligned}
0 &= C_1 \frac{d(U_0 - U_1)}{dt} - (U_{in} - U_0)G_0 \\
0 &= (U_{in} - U_0)G_0 - (U_1 - U_B)G_B - (U_1 - U_{g1})G_{g1} \\
0 &= (U_1 - U_{g1})G_{g1} - i_g
\end{aligned}
\tag{24}
$$

where the U_b is the bias voltage and U_{in} are inverted input signals. Then the plate voltages are computed from

$$
\begin{aligned}
0 &= -i_{a1} + (U_D - U_{a1})G_{a1} \\
0 &= -i_{a2} + (U_D - U_{a2})G_{a2} \\
0 &= -i_{s1} + (U_D - U_{s1})G_{s1} \\
0 &= -i_{s2} + (U_D - U_{s2})G_{s2} \\
0 &= -i_{a1} - i_{a2} - i_{s1} - i_{s2} + (U_N - U_D)G_D - \\
& \quad - C_2 \frac{dU_D}{dt}
\end{aligned}
\tag{25}
$$

and finally, the output signal is obtained from

$$
U_{OUT} = \frac{U_{a1} - U_{a2}}{N}
\tag{26}
$$

where N is the output transformer ratio.

7.1. Approximation of Differential Equations

The approximated functions for the grid current circuit are

$$
\begin{aligned}
U_g &= U_{Gapprox}(U_{in}, U_{c1m}) \\
U_1 &= U_{1approx}(U_{in}, U_{c1m})
\end{aligned}
\tag{27}
$$

and the capacitor voltage is recomputed using

$$Uc_{1m}[n+1] = Uc_{1m}[n] -$$
$$- \frac{(U_1 - U_B)G_b + (U_1 - U_{g1})G_g}{C_1 f_s}. \qquad (28)$$

The approximated functions for the plate current circuit are

$$U_{A1} = U_{A1approx}(U_{g1}, U_{g2}, U_{c2m})$$
$$U_{S1} = U_{S1approx}(U_{g1}, U_{g2}, U_{c2m})$$
$$U_{A2} = U_{A2approx}(U_{g1}, U_{g2}, U_{c2m}) \qquad (29)$$
$$U_{S2} = U_{S2approx}(U_{g1}, U_{g2}, U_{c2m})$$

and the new capacitor voltage is obtained from

$$Uc_{2m}[n+1] = Uc_{2m}[n] +$$
$$+ \frac{(U_N - U_{c2m})G_d - (i_{a1} + i_{a2} + i_{s1} + i_{s2})}{C_2 f_s}. \qquad (30)$$

7.2. Simulation Results

The push-pull power amplifier with two 6L6GC tubes was simulated with the input 1 kHz sinewave signal with an amplitude of 200 V and a sampling frequency of 96 kHz. Firstly, the opposite grid voltages were computed from the grid current circuit. Subsequently, these voltages were used as inputs for the plate current circuit. The output signal from the amplifier is shown in Figure 16. One can see the symmetrical signal limiting, which is typical for power amplifiers and also the output signal amplitude compression (sagging effect) can be seen in Figure 16. The power supply drops due the current flowing through the resistor R_D and the level of the output voltage decreases while the input signal has the same amplitude.
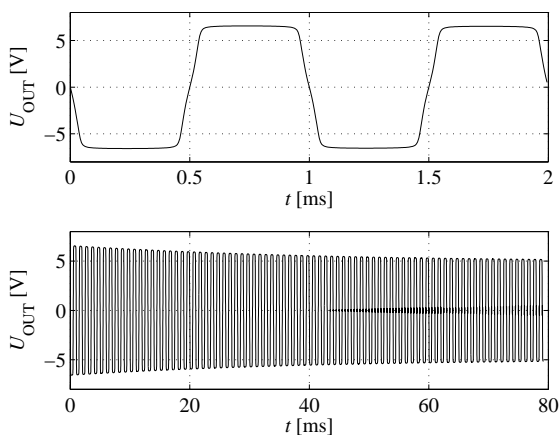
Figure 16: *The output signal from the output transformer – symmetrical limiting (top), compression effect (bottom).*

8. SPEAKER CABINET SIMULATION USING IMPULSE RESPONSE APPROXIMATION

Complete guitar amplifier simulation was described in previous sections. However, the amplifier can not work without the loudspeaker and the loudspeaker dramatically affects the color of the resulting sound as well. Hence the speaker simulation algorithm has to be involved in guitar amplifier simulation. Good results are obtained using filtration with measured impulse responses. The impulse responses were measured with varied positioning of the measuring microphone in front of the loudspeaker and subsequently, the measured impulse responses were interpolated using bilinear interpolation to simulate any position of the microphone in front of the loudspeaker. The frequency response for the measured Mesa Boogie speaker cabinet is shown in Figure 17 top and the detailed frequency responses for neighboring positions are displayed in Figure 17 bottom (the dash-dotted and dashed lines show measured frequency response and the solid line shows the interpolated one). The step of the measuring grid was 2 cm.
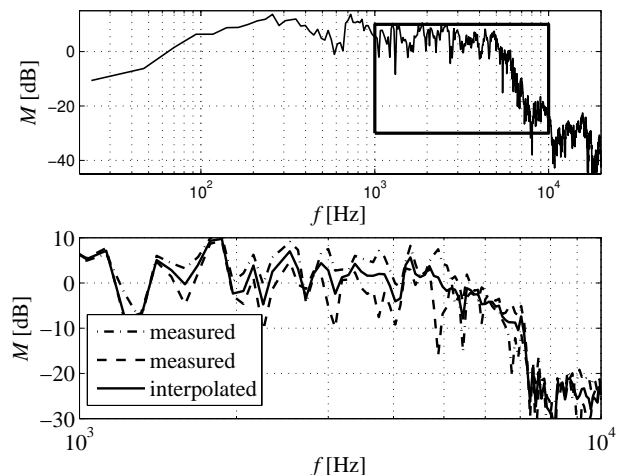
Figure 17: *Frequency responses of measured Mesa Boogie speaker cabinet.*

9. REAL-TIME IMPLEMENTATION

The algorithms were implemented in C++ language as the VST plug-in effect. IIR filter was used for the tone stack simulation and the FDL (frequency-domain delay line) convolution was chosen for the loudspeaker cabinet simulation [9]. The major advantage of the FDL convolution is low latency with low computational complexity. Several famous guitar amplifiers were simulated (e.g., Marshall and Mesa Boogie). Sound examples are available on the web page www.utko.feec.vutbr.cz/~macak/ DAFx10/. The amplifiers were decomposed according to the previous chapters and each part was described by the ODEs and then approximated. The real values of the circuit elements and also the topology depend on the particular amplifier. However, the circuits shown in this paper are very similar to the original ones. The computational complexity of the simulation algorithm is constant, the output signal value and the new capacitor values are computed using approximating functions. Therefore, the computational complexity depends on the chosen approximation technique. The lowest computational complexity is achieved when linear approximation is used. However, a large resolution of the look-up table for linear approximation has to be used for smooth behavior of the approximated function. Therefore, the spline approximation was used for this simulation. The simulation using approximation were

compared to the solution of the ODEs and all results were similar to the Figure (5). The maximal error was about 2% of the maximum signal level for 2 V step of input and capacitor voltages.

The algorithms were tested in real-time with a 1.6 GHz PC with 512 MB RAM at a sampling frequency of 48 kHz with 2-x oversampling (polyphase FIR interpolation). The total computational complexity especially depends on the number of simulated tubes (for four preamp tubes, the phase splitter and the push-pull amplifier is about the 58 % of CPU load). The algorithm implementation is not optimized very well. The nonlinear tube models are implemented according to (1),(3),(5) and (6) and can be replaced with the look-up table.

10. CONCLUSIONS AND FUTURE WORK

The appropriate division of complete guitar tube amplifier into separated blocks was found, the individual blocks were described and the resulting equations were approximated. The major advantage of the approximation is constant computational complexity and the stability of the algorithm compared to algorithms that use numerical algorithms for solving the implicit nonlinear functions (e.g., K-method [3] or solution of ODEs without approximation). This solution also enables more nonlinear functions without adding computational load. The major disadvantage is a bounded number of accumulation elements in the circuit schematic because the dimension of approximating functions increases with the number of accumulation elements, which is related to the memory demands and the computational complexity increases as well.

Future work is related to improving of the push-pull amplifier and output transformer models. The approximation of the other methods will be investigated as well.

11. ACKNOWLEDGMENTS

12. REFERENCES

[1] J. PAKARINEN and D. T. YEH, "A review on digital guitar tube amplifier modeling techniques," *Computer Music J.*, vol. 33, no. 2, pp. 85–100, Jun. 2009.

[2] T. D. Yeh, J. S. Abel, and J. O. Smith, "Simplified, physically-informed models of distortion and overdrive guitar effects pedal," in *Proc. Digital Audio Effects (DAFx-07)*, Bordeaux, France, Sep. 10-15, 2007, pp. 189–196.

[3] T. D. Yeh and J. O. Smith, "Simulating guitar distortion circuits using wave digital and nonlinear state-space formulations," in *Proc. Digital Audio Effects (DAFx-08)*, Espoo, Finland, Sept. 1-4,, 2008.

[4] J. Pakarinen and M. Karjalainen, "Wave digital simulation of a vacuum-tube amplifier," in *Proc. Intl. Conf. on Acoustics, Speech, and Signal Proc.*, Toulouse, France, May 15-19, 2006.

[5] J. Pakarinen, M. Tikander, and M. Karjalainen, "Wave digital modeling of the output chain of a vacuum-tube amplifier," in *Proc. of the Int. Conf. on Digital Audio Effects (DAFx-09)*, Como, Italy, Sept. 1–4, 2009.

[6] T. D. Yeh, J. S. Abel, and J. O. Smith, "Simulation of the diode limiter in guitar distortion circuits by numerical solution of ordinary differential equations," in *Proc. Digital Audio Effects (DAFx-07)*, Bordeaux, France, Sep. 10-15, 2007, pp. 197–204.

[7] David T. Yeh and Julius O. Smith, "Discretization of the '59 Fender Bassman tone stack," in *Proc. of the Int. Conf. on Digital Audio Effects (DAFx-06)*, Montreal, Quebec, Canada, Sept. 18–20, 2006.

[8] N. Koren, "Improved vacuum tube models for SPICE simulations," Available at http://www.normankoren. com/Audio/Tubemodspice_article.html, 2003.

[9] G. García, "Optimal filter partition for efficient convolution with short input/output delay," in *Proc. of the AES 113th Convention*, Los Angeles, California, USA, October 2002.

[10] D. G. Manolakis and J. G. Proakis, *Digital Signal Processing: Principles, Algorithms and Applications*, Prentice Hall, Englewood Cliffs, NJ, USA, 3rd edition, 1991.

[11] T. Serafini S. Barbati, "A Perceptual Approach on Clipping and Saturation," Available at http:// www. simulanalog.org/clip.pdf, 2002.

[12] U. Zölzer, *DAFX - Digital Audio Effects*, J. Wiley & Sons, Ltd, 1st edition, 2002.